

Experiment of Stability Operation Region and MHD Instability Observation on HT-7

ZHAO Qingchu*, CHEN Lei and the HT-7 Group
Institute of Plasma Physics, Academia Sinica
P.O.Box 1126, Hefei, Anhui 230031, P.R.China

(Received: 30 September 1997/Accepted: 5 February 1998)

Abstract

Experiments about stability operation region (SOR) on HT-7 and high plasma parameters in Ohmic discharge are performed. Two boundaries of low density limit and Murakami density limit are scanned out through about 80 shots. The Murakami limit $M_{\max} = 2.96 \times 10^{19} \text{ m}^{-2}/\text{T}$ and Hugill number $H = 9.5 \times 10^{19} \text{ m}^{-2}/\text{T}$ are obtained. On the Murakami boundary, the radiation characters are specially analyzed. Coupling of $m=1$ and $m=2$ modes leads impurities from boundary to core, then line radiation of those impurities causes energy quenching inside and near $q=1$ surface and finally disruption occurs. This kind of disruption restricts Murakami density limit.

Keywords:

stability operation region, Murakami density limit, Hugill plot, tearing mode coupling, central impurity, line radiation, energy quenching, disruption

1. Introduction

The Murakami limit was first proposed as an empirical scaling for the highest density achievable[1]. This density limit has been attributed to a loss of balance between input and radiated power. The Hugill scaling was proposed from DITE ohmic and additionally heated discharges. Hugill plot is used to show the accessible operation region of a tokamak for density and current[2]. A slightly different scaling was derived by Greenwald from comparison of several different machines[3]. Up to now, understanding the power independent, $1/q$ -type scaling (Hugill-Greenwald type scaling) is still interesting[4].

There have been five operation phases on HT-7 from December of 1995 to June of 1997. We wonder what an accessible operation region, radiating extent, the most achievable density and high parameters on HT-7 are.

2. Experiment about SOR

According to Hugill scaling and our obtained data on HT-7, the SOR is designed. First ohmic-heating-field's voltage is fixed. In order to scan the density, the amplitude and the pulse time of gas puffing are adjusted respectively. Then the above voltage is changed to scan the current. The obtained SOR is close to our designing one. However if Z_{eff} is lower or the ramp-up rate of \bar{N}_e is suitable, the SOR is expanded; otherwise SOR is reduced. In Hugill plot (Fig.1) we get the following parameters:

Hugill number : $H = 9.5 \times 10^{19} \text{ m}^{-2}/\text{T}$

$$(H = \bar{N}_e q_a R / B_T),$$

Murakami number : $M_{\max} = 2.96 \times 10^{19} \text{ m}^{-2}/\text{T}$

$$(M = \bar{N}_e R / B_T).$$

According to Greenwald limit scale, we obtained normalized density: $(\bar{N}_e \pi a^2 / I_p)_{\max} = 0.72 \times 10^{20} \text{ m}^{-1}/\text{MA}$. In this experiment, the maximum values of other parameters are $I_p = 205 \text{ kA}$, $\bar{N}_e = 4.97 \times 10^{19} \text{ m}^{-3}$, $B_T =$

*Corresponding author's e-mail: qczhao@ipnc1.hfcas.ac.cn

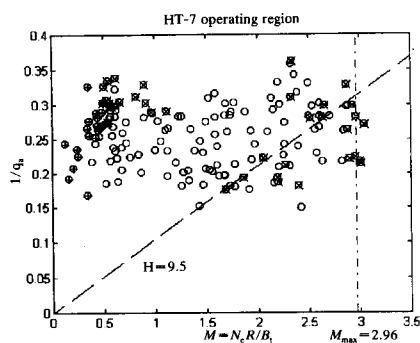


Fig. 1 Hugill plot on HT-7 obtained from about 80 shots in ohmic SOR experiment.

× -- Instability point, + -- Run away point
 ○ -- Stability point
 N_e -- Average electron density of central chord
 R -- Major radius, B_t -- Toroidal field
 q_a -- Boundary safety factor
 M (Murakami number) = $N_e R / B_t$ ($10^{19} \text{m}^{-2} \text{T}^{-1}$)
 H (Hugill number) = $N_e q_a R / B_t$ ($10^{19} \text{m}^{-2} \text{T}^{-1}$)

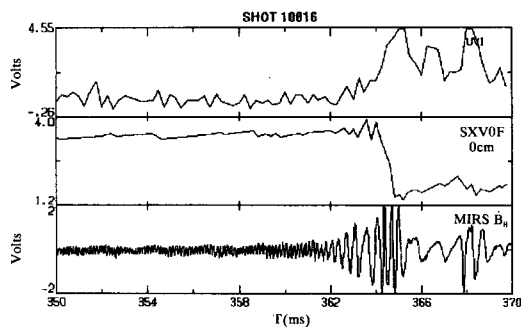
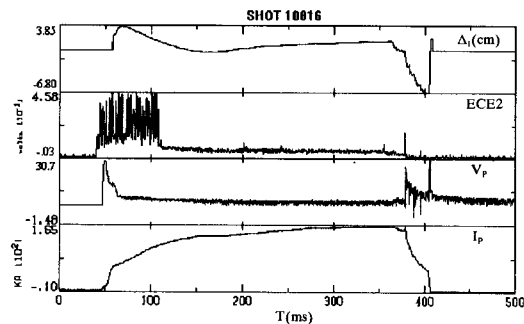
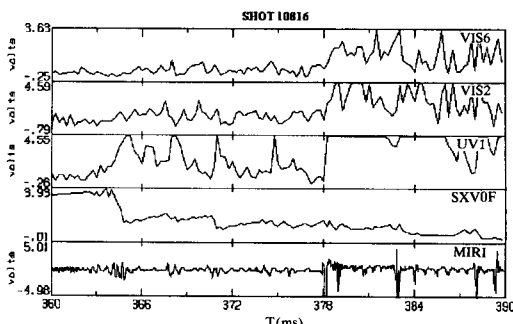


Fig. 2 Energy quenching process caused by line radiation.

The $m=2$ mode begins to grow at about $t=362$ ms and couples with $m=1$ mode until 364 ms. Tendency of the soft X-ray intensity's dropping and BIV radiation's rising is coincident from 364 ms to 364.8 ms.



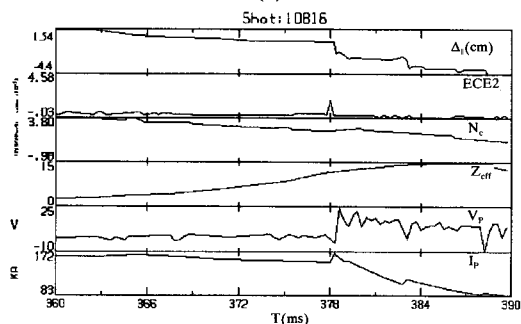
(a)



(b)

Fig. 3 All processes from energy quenching ($t=364$ ms) to disruption ($t=378$ ms).

ECE2: ECE 11.3 cm
 VIS6: CIII 15.6 cm
 VIS2: CIII 3.1 cm
 UV1: BIV 0 cm
 SXV0F: Soft X-ray intensity 0 cm
 MIR1: B_θ



(c)

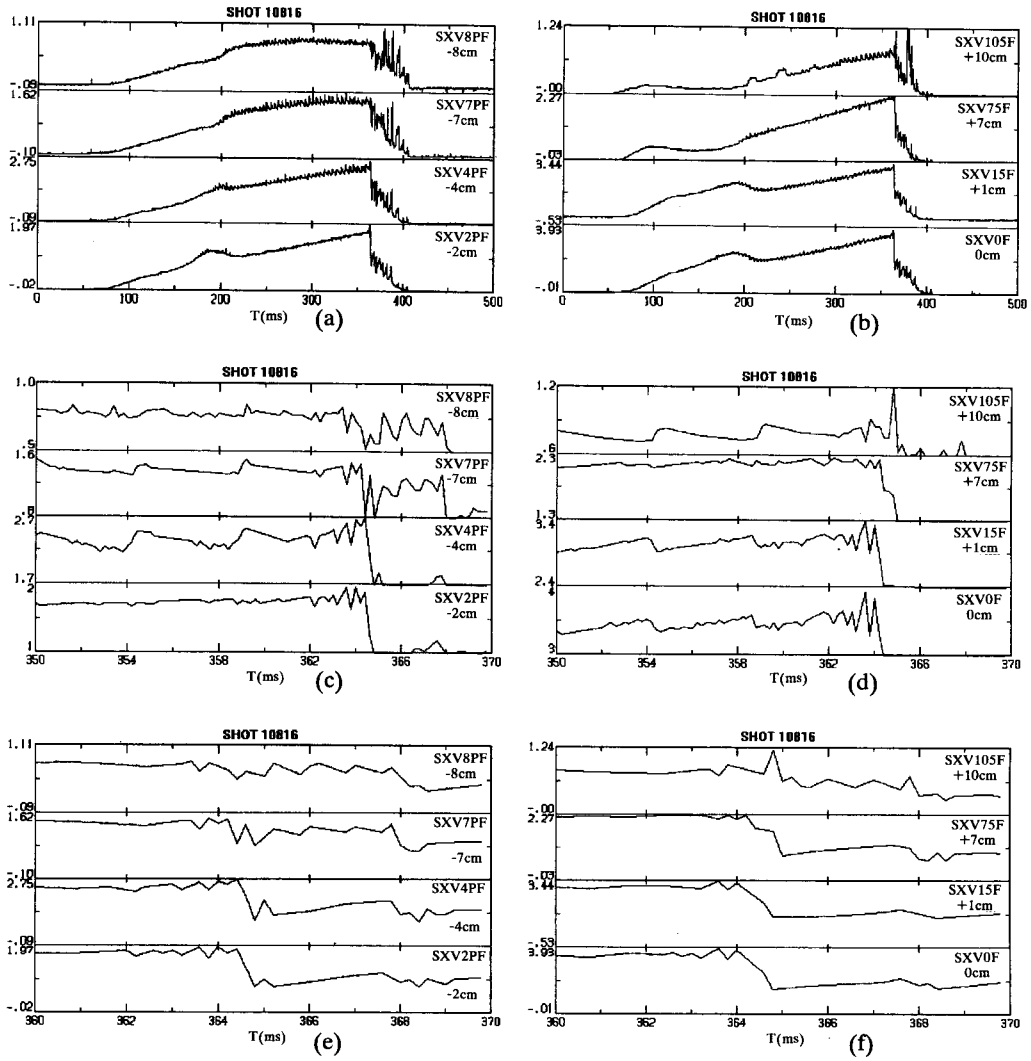


Fig. 4 Spatial region and sequence of energy quenching are shown from soft X-ray chord intensity.

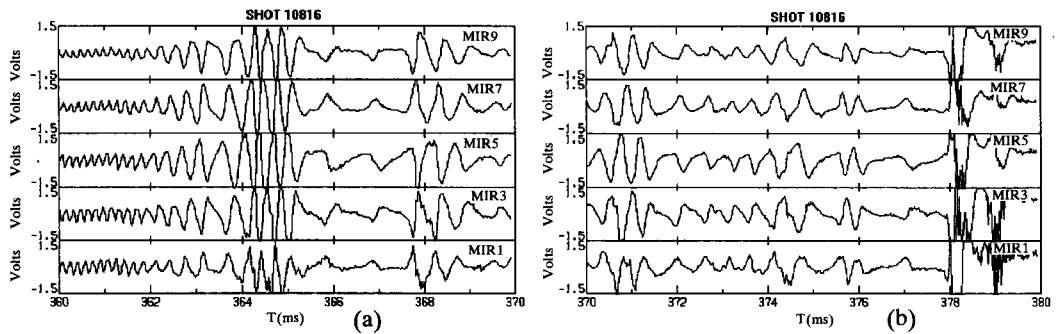


Fig. 5 (a) Increasing of the $m=2$ mode frequency during energy quenching (from 364 ms to 364.8 ms) is shown.
 (b) Disruption occurs at $t=378$ ms.

2.09 T.

Abundant MHD phenomena are observed in this experiment. Along constant q^{-1} line in Hugill plot, MHD activities pass different phases: without MHD mode, MHD mode generating, MHD mode growing, mode saturating, mode locking and hard disrupting. Rotating frequency of MHD modes is changed during one shot or in different shots.

3. Understanding the Hugill Plot (HP)

The q_a^{-1} , ordinate of HP, presents boundary's parameter apparently but profile-average's parameter practically. It is easy to deduce $q_a^{-1} = \pi/5 * (\bar{j}R/B_T)$, \bar{j} is average current density.

Every point in Hugill plot is only corresponding to average value \bar{j} and \bar{N}_e . On the same point, average values are the same, while profile parameters ($j(r)$, $n(r)$) can be different. So a point in stability operation region may be an instability point, which is determined by discharge conditions, for example, gas pulse rate and plasma displacement adjusting, etc. Therefore boundaries of Hugill plot show only the most realizable stability operation region of a tokamak.

4. Line Radiation of Central Impurity Restricts Murakami Limit on HT-7

From comparison of Hugill plot with boronized wall (Ohmic discharge) between TEXTOR[5] and HT-7, there is smaller Murakami limit on HT-7. One of the differences between the two devices is graphite limiters and stainless steel limiters.

Radiation and disruption process of a shot on Murakami limit are analyzed. Seeing Fig.2, $m=2$ mode begins to grow at about $t=362$ ms. Then the frequency slows down. Meanwhile the amplitude increases, which can be seen from soft X-ray intensity (SXV0F, $r=0$ cm). When the amplitude of $m=2$ mode approaches some extent, the coupling of $m=1$ and $m=2$ modes occurs. This type of coupling was studied in detail through drawing the sequence of soft X-ray tomographic images during the precursor $m=1$ and $m=2$ modes in T-10[6]. We consider that mode's coupling leads to reconnection of magnetic field and enhances radial particle transport. Therefore boundary's impurities (including heavy impurity) move towards the high temperature core. Intense line radiation of the impurities in the core results in energy quenches inside and near $q=1$ surface. Seeing Fig.2, the tendencies of soft X-ray intensity's dropping and BIV radiating power's rising are coincident from 364 ms to 364.8 ms. In Fig.4(c)(d), the $q=1$ reverse surface is at $r=+7.5$

cm and $r=-2$ cm. The sudden dropping occurs mainly from $+7.5$ cm to -4 cm. In Fig.4(e)(f), spatial sequence of the dropping is from center (0 cm, $+1$ cm) to outside ($+7$ cm), finally to inside (-2 cm, -4 cm). During the dropping process (about 800 μ s), central hollow profile is formed, the frequency of $m=2$ mode is increased (seeing Fig.2 and Fig.5(a)), plasma current is increased a little, toroidal voltage is not changed, horizontal displacement is towards inside (in Fig. 3(c)). Although this energy quenching occurs inside and near $q=1$ surface only and does not lead to disrupting of $m=2$ island temporally, disruption occurs finally at $t=378$ ms. At the same time, CIII line increases and BIV line bursts, seeing Fig.3(c), Fig.3(b). For the plasma temperature at 378 ms is much lower than the one ($T_e(0) \approx 800$ eV) at 364 ms, while BIV line appears at so low temperature at 378 ms, the existence of other impurity line radiation at $t=364$ ms is supposed.

5. Summary

Many experimental evidences, which prove that the coupling of $m=1$ and $m=2$ modes causes boundary impurity to move towards center and the central impurity-line-radiation leads to energy quenching, are obtained on HT-7. This kind of process restricts Murakami density limit.

References

- [1] M. Murakami *et al.*, Nucl. Fusion **16**, 347 (1976).
- [2] K.B. Axon *et al.*, *Plasma Physics and Controlled Nuclear Fusion Research*, 1980 (*Proc. 8th Int. Conf. Brussels*, 1980), Vol.1, IAEA, Vienna, p.413 (1981).
- [3] M. Greenwald *et al.*, Nucl. Fusion **28**, 2199 (1988).
- [4] K. Borrass and R. Schneider, Nucl. Fusion **37**, 523 (1997).
- [5] G. Waidmann and G. Kuang, Nucl. Fusion **32**, 645 (1992)
- [6] D.A. Kislov *et al.*, in *Controlled Fusion and Plasma Heating (Proc. 17th Eur. Conf., Amsterdam*, 1990), Vol.14b, Part 1, European Physical Society, 315 (1990).